International Journal of Engineering and Science Invention (IJESI)
ISSN (Online): 2319-6734, ISSN (Print): 2319-6726
www.ijesi.org ||Volume 13 Issue 12 December 2024 || PP 08-16

Effect of oxalic, nitric and ascorbic acids on the supercapacitance of hydrothermally synthesized 1T/2H MoS_2 nanoflowers

Ajay Kumar[1*], Manisha[1], Divya Deep Yadav[1,2], Ranjana Jha[1]
[1]*Research Lab for Energy Systems, Department of Physics, N.S.U.T, Dwarka, New Delhi-110078, India.*
[2]*Ramjas College, University Enclave, University of Delhi, Delhi-110007, India.*
** Corresponding author*

Abstract:
MoS_2 has drawn much attention towards energy storage devices in recent years due to its high conductivity and good catalytic activity for electrochemical devices. 3D nanoflowers of 1T/2H MoS_2 with different particle sizes were synthesized using facile hydrothermal method. Oxalic acid, nitric acid, and ascorbic acids were used during the synthesis method other than Mo and sulfur source, to study the effect on morphology, surface area, and electrochemical activity. X-ray Diffraction (XRD), Field Emission Scanning Electron Microscopy (FESEM), High Resolution Transmission Electron Microscopy (HRTEM) and UV-Vis Spectroscopytechnique were used to study the structure, morphology and band gap energy of synthesized nano powders. MoS_2 nanoflowers formed using ascorbic acid as a precursor showed high specific capacitance(229 F/g) than other synthesized samples. Structural morphological and electrochemical results showed that MoS_2nanostructure material formed with ascorbic acid as a reducing agent can be suitable electrode materials for electrochemical supercapacitorsdevices in the future.

Keywords: *Energy storage devices, electrochemical supercapacitor, electrode, electrolyte, nanoflower*

I. Introduction

Coal, crude oil, and natural gases are energy resources used widely in industry. Due to the daily use of these resources on a large scale, a shortage of these fossil fuels will occur in the future. These fossil fuels also cause environmental pollution. Therefore, some alternatives to these fossil fuels are needed in the future to resolve the energy crisis and environmental pollution issues. Renewable energy resources such as solar energy, wind energy, and hydro energy resolve the energy need and pollution problems[**1,2].** But due to high cost and low output of energy, application of these resources is limited. In recent years, electrochemical energy storage has attracted the focus of researchers to resolve the energy crisis issue in the future. Battery and supercapacitors are the two main energy devices that are capable of providing clean energy. Batteries have low power density, limiting charging/discharging life cycle, and high cost as compared to supercapacitors**[3].** Therefore, supercapacitors are the ones to fulfil the energy need. Supercapacitors are mainly divided into two classes: pseudo-capacitors and electric double-layer capacitors, based on their charge storage mechanism. Hybrid capacitors are also made using these two types of capacitors. In EDLCs, charge storage occurs only on the surface of the electrode, and the mechanism is non faradic, while in supercapacitors, faradic redox processes occur at and near the surface of the electrode**[4].**

Variable oxidation state, eco-friendliness, and stability towards redox reactions of the transition metal sulfide/oxide/diseleniums, metal hydroxides, and conducting polymers make them a promising electrode material for supercapacitor applications**[5].** Among these TMS are advanced materials for supercapacitor due to their high electrical conductivity, large surface area, low cost, and excellent performance towards redox reactions at the electrode-electrolyte surface. Commonly used sulfides for supercapacitors are nickel sulfide, manganese sulfide, molybdenum disulfide, cobalt sulfide, zinc sulfide, and iron sufide**[6].** Among these TMS, MoS_2 draws much attention from researchers due to their unique properties like optical, chemical, mechanical, electrocatalytic, and photocatalytic. MoS_2 is widely used in energy storage devices, sensors, photocatalytic degradation of dyes, light-emitting diodes, photodetectors, **etc. [7].** The crystalline structure of MoS_2 exists in three phases: 2H MoS_2 is stable, 3R is unstable, and 1T is metastable. The conductivity of the 1T phase of MoS_2 is 10^5 times higher than that of the 2H semiconducting phase and has more active sites than 2H MoS_2**[8].**MoS_2 consists of a layered structure of S-Mo-S, connected via weak Vander wall forces while atoms are connected through strong covalent bonds. In MoS_2, exposed surface or active sites lie along the S-Mo-S layer (known as basal planes (002)) or along the edge of S-Mo (known as edge sites plane (100)). Edge sites are highly active towards electrochemical properties than basal plane sites**[9].** Properties of 2H MoS_2 can be enhanced by forming composites, heterostructures, mixed phases with 1T MoS_2, etc. 2H phase mixed with 1T phase results in 1T/2H structure, which is highly conducting and has more active sites as compared to 2H phase. Various synthesis

methods, such as chemical vapor deposition, sol-gel, evaporation, exfoliation, solvothermal, and hydrothermal, are used for the preparation of 1T/2H MoS_2. Among these hydrothermal methods is cost-effective and most facile to synthesize various structures of MoS_2 with high crystallinity.Lina N Khandareet al. reported that MoS_2 nanobelts/Carbon hybrid were synthesized using the hydrothermal method at 220^0 C for the supercapacitance applications, with a specific capacitance reaching a value of 77.5 farad/g**[10].** Kamal has reported that the hydrothermally synthesized 1T/2H-O-MoS_2@GFwith enhanced active sites was used for the supercapacitor and showed aspecific capacitance value of 280F/g at 1A/g.**[11].**

Herein 1T/2H MoS_2 nanoflowers were hydrothermally synthesized using different precursors. The precursors used here are sodium molybdate dihydrate for Mo sources, thiourea as a sulfur source in all three synthesized samples, and three different acids, oxalic, nitric, and ascorbic, are used to alter the morphology and other various parameters. The effects of oxalic acid, nitric acid, and ascorbic acid were seen on the structural, morphological, and electrochemical activities. XRD, FESEM, HRTEM and UV Visible techniques were used to identify the structure, morphology and band gap energy of synthesized samples. Electrochemical measurements were done for the comparison of the specific capacitance of synthesized samples. The result of electrochemical analysis shows that the material electrode formed using ascorbic acid has much better specific capacitance and possesses a large surface area as compared to the other two electrodes formed using oxalic and nitric acids.

II. Chemical used

Sodium molybdate dihydrate and thiourea are purchased from the Sigma-Aldrich company. Oxalic acid, nitric acid, and ascorbic acid are purchased from LobaChemie. All chemicals are directly used during the synthesis process without any further purification.

2.1 Synthesis method:

A facile hydrothermal process was used to prepare 1T/2H MoS_2nanostructures. Firstly1.8gmof sodium molybdate dihydrate and 4.7gmof thiourea were dissolved in 100 ml of DI water and left for magnetic stirring at a speed of 500 rpm for 0.5 hour. Further1.3 gmof oxalic acid was further added into the solution and left the solution under magnetic stirring for 1 hour. The mixture was poured into a 200-ml autoclave and kept in a hot air oven at 200^0 C for 25 hours. After natural cooling at room temperature, the centrifugation process of the obtained powder was done using DI and ethanol several times to remove waste products. Afterwards, the obtained powder was further kept in a vacuum oven at 60^0C for 24 hours. Another two 1T/2H nanostructures were also synthesized using the same process as discussed above by using nitric and ascorbic acid instead of oxalic acid in the same amount. These samples are denoted using the notation MoS_2 (O), MoS_2 (N), and MoS_2 (A) for oxalic, nitric, and ascorbic acid, respectively.

2.2 Characterization technique:

An X-ray diffractometer (Bruker, D8 Discover,X-ray source Cu, 3KW) equipped with Cu Kα radiation (1.54 A) was used to analyze the crystallinity and crystal structure of synthesized nanostructures. Field emission transmission electron microscopy (Zeiss GeminiSEM 500 Thermal field emission type, Acceleration voltage 0.02 – 30kV, Probe current 3 pA – 20nA and Magnification 50x – 2,000,000x) was used to study the morphology of nanostructures, and EDAX attached with the fesem was further used to study the elemental composition of material. Interlayer spacing and high-resolution images up to 10 nm were obtained from high resolution field emission transmission electron microscopy (HRTEM,Tecnai, functioning at 200 kV). UV visible diffuse reflectance spectroscopy was conducted using a Shimazdu 240 spectrometer with a wavelength range from 190 nm to 900 nm.

2.3 Preparation of electrode:

20 mg of synthesized powder were taken into 1ml of distilled water for the preparation of the working electrode as used in electrochemical analysis. 90 ul of Criton X was added to the solution. Here criton X acts as a binder, which plays a major role in binding the particles of synthesized powder. After that, the solution was kept in an ultrasonic bath for 3 hours to form a homogeneous solution. To prepare the working electrode, nickel foam was used. Firstly, nickel foam was cleaned and then used for the working electrode. To clean nickel foam, 1M of HCL solution was taken into a beaker, and nickel foam was dipped into it for 20 minutes. After that, nickel foam was rinsed with DI water. The same process was repeated in acetone and then in DI water to clean nickel foam. Finally, the homogenous solution drops onto the cleaned nickel foam. The nickel foam coated with material was then heated in a vacuum oven at 60 C for 10 hours. The obtained nickel foam was further used as the working electrode. Electrochemical Workstation: “SP-240 Biologic with a three-electrode configuration was used to analyze the electrochemical properties of prepared electrode material. Here in electrochemical analysis, platinum and calomel electrodes were used as counter and reference electrodes.

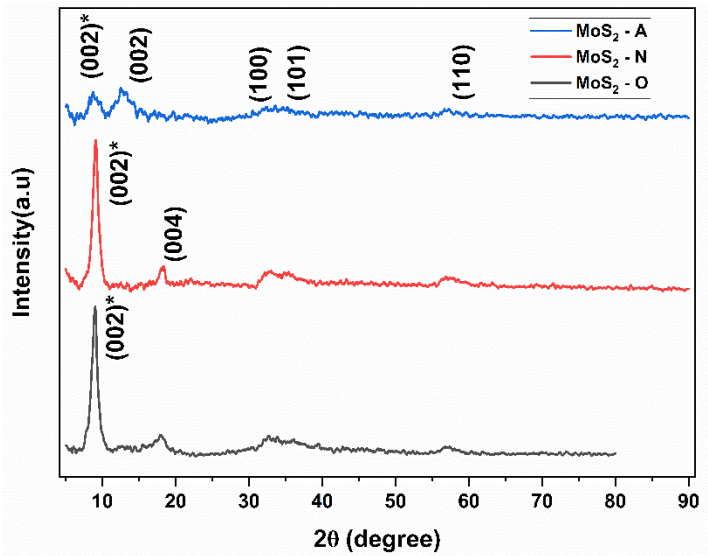

Figure 1:XRD pattern of (a) MoS_2-O,(b) MoS_2-N and (c) MoS_2-A

III. X-Ray Diffraction (XRD) analysis

Figure 1 show the x-ray diffraction pattern of as synthesized nanostructured named MoS_2 (O), MoS_2(N) and MoS_2(A). Diffraction peak located at 9^0,13^0,18^0,32.7^0,35.2^0 and $57.3^0$are arisen due to lattice plane (002) *, (002), (104),(100), (102), and (110) respectively. The diffraction peak located at 9 is arise due to (002) * plane which corresponds to 1T phase of MoS_2.Peak located other than 9 are arise due to 2H phase of MoS_2These diffraction peaks are well matched with the JCPDS card00-037-1492 confirming the 1T/2H phase of MoS_2. The interlayer d spacing of all three prepared sample are calculated using the Bragg equation which is**[12]**

---------- (1)

Where, θ = Bragg's angle
d = interplanar spacing
λ = 0.154nm is the X-ray wavelength

The obtained values at an angle of 9^0 are 0.97, 0.96, and 1 nm, corresponding to MoS_2 (O), MoS_2 (N), and MoS_2 (A), respectively.The d spacing value at angle 14^0 in sample MoS_2(A) has values of 0.4nm.These results confirmed that the sample MoS_2 (O), MoS_2(N) and MoS_2(A) consists of 1T/2H phase of MoS_2.The broad diffraction peak at 9^0 and 14^0 showed that the crystal structure is nanocrystalline in nature. The crystallite size of nanostructures at 9^0 is calculated using Scherrer's formula(equation 2),which is

----------(2)

where,
K = 0.9 is the crystallite shape factor,
λ = 0.154nm is the X-ray wavelength,
β = full width at half maximum
θ = Bragg's angle

The crystallite sizes of MoS_2 (O), MoS2 (N), and MoS2 (A) are 9.3 nm, 9.40 nm, and 4.79 nm, respectively.

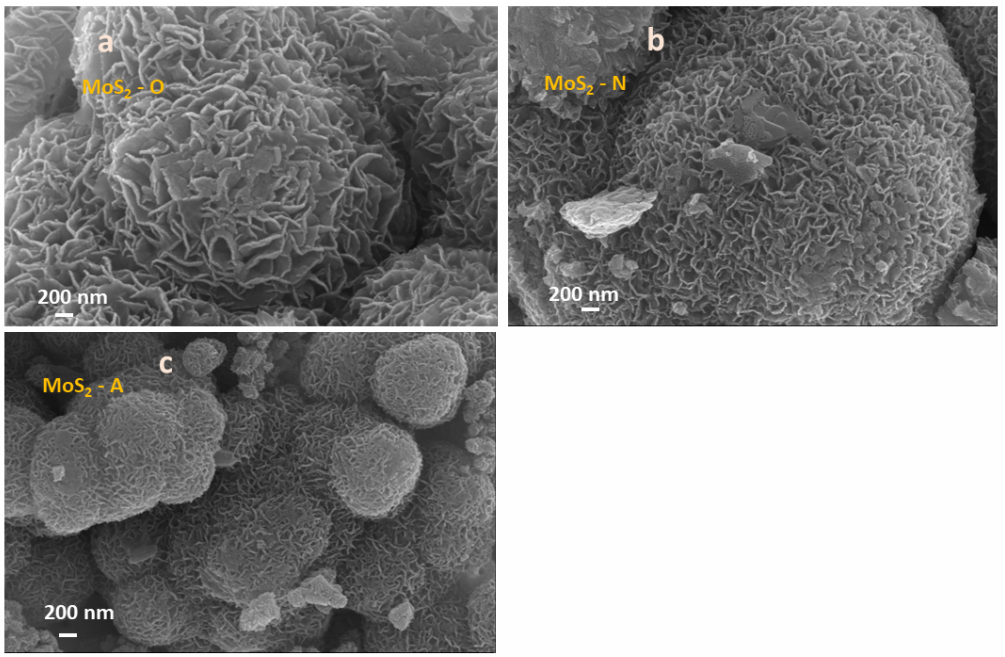

Figure 2:FESEM images of (a) MoS_2-O, (b) MoS_2-N and (c) MoS_2-A

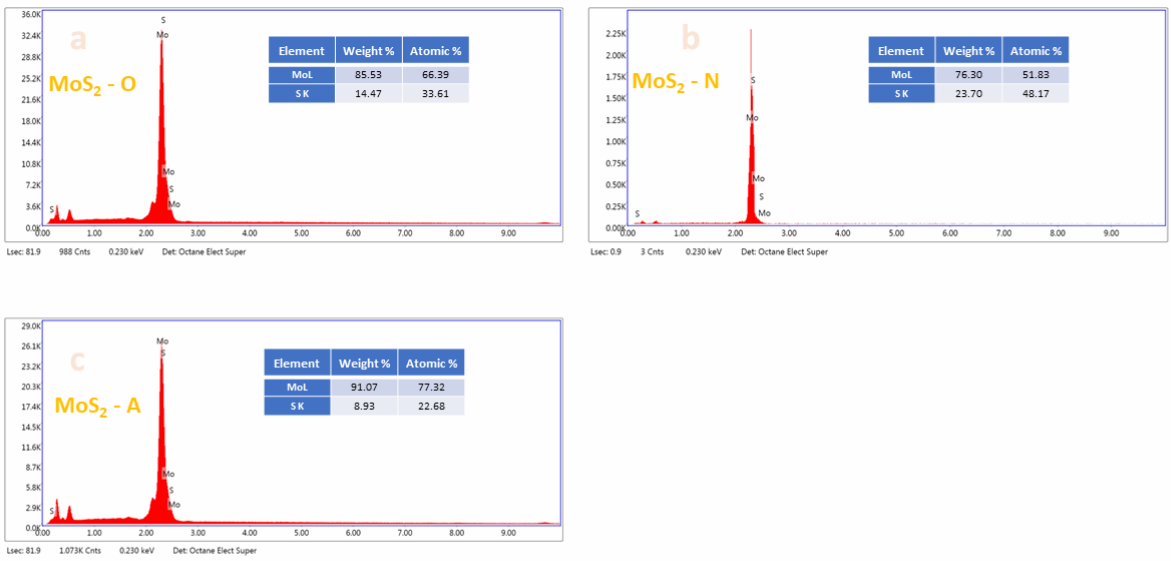

Figure 3:EDX spectra of (a) MoS_2-O, (b) MoS_2-N and (c) MoS_2-A

IV. Field Emission Scanning Electron Microscopy (FESEM) and Energy Dispersive X-ray (EDX) analysis

FESEM analysis is used to study the morphology of synthesized samples. FESEM analysis showed that the nanosheets agglomerated to form the nanoflower like shape of all three samples named MoS_2 (O), MoS_2(N) and MoS_2(A)(fig.2). The effect of oxalic, nitric acid and ascorbic acid is to change the size and shape of nanoflowers, as shown in figure (2). The nanoflower formed with ascorbic acid is highly porous as compared to others. The particle size values of these nanoflowers are 2.4 µm for MoS_2(O), 3.8 µm for MoS2(N), and 1 µm for MoS_2(A), respectively.EDX spectra of the synthesized sample showed elements present in the MoS_2 (O), MoS_2(N) and MoS_2(A) nanostructures. Figure 3 depicts the FESEM EDX spectra, which show that only molybdenum and sulfur are present in the samples. No other elements were detected, showing the purity of MoS_2 formation.

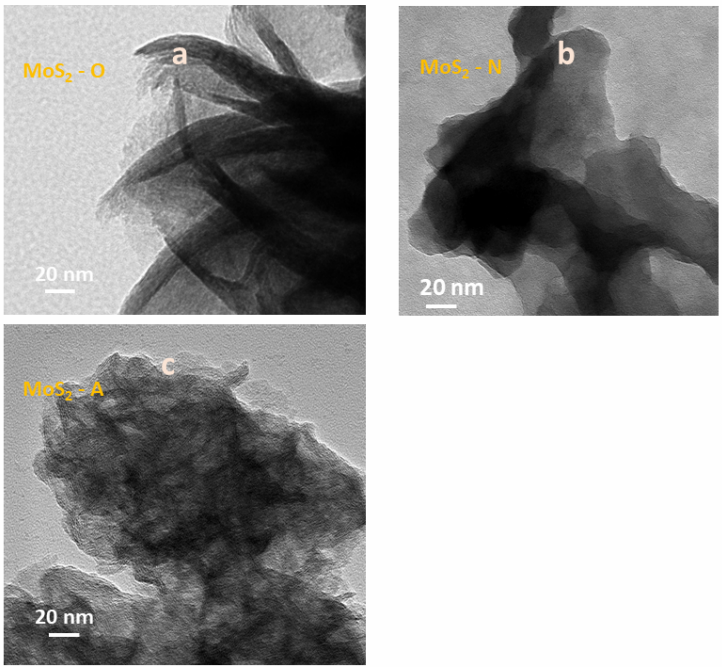

Figure 4:HRTEM images of (a) MoS_2-O, (b) MoS_2-N and (c) MoS_2-A at 20 nm

V. High Resolution Transmission Electron Microscopy (HRTEM) analysis:

To further study the crystallinity of synthesized samples, HRTEM analysis was used. Figure4 showed that the low magnification imagesdepict the different layers of MoS_2 nanosheets of (a) MoS_2-O, (b) MoS_2-N and (c) MoS_2-A at 20 nm**.** The nanosheets are cross linked to each other. Further the d spacing values from these lattice images are to be 0.97, 0.96, and 1 nm for MoS_2 (O), MoS_2(N) and MoS_2(A) respectively. These interplanar spacing values agreed with the values obtained from the XRD pattern.

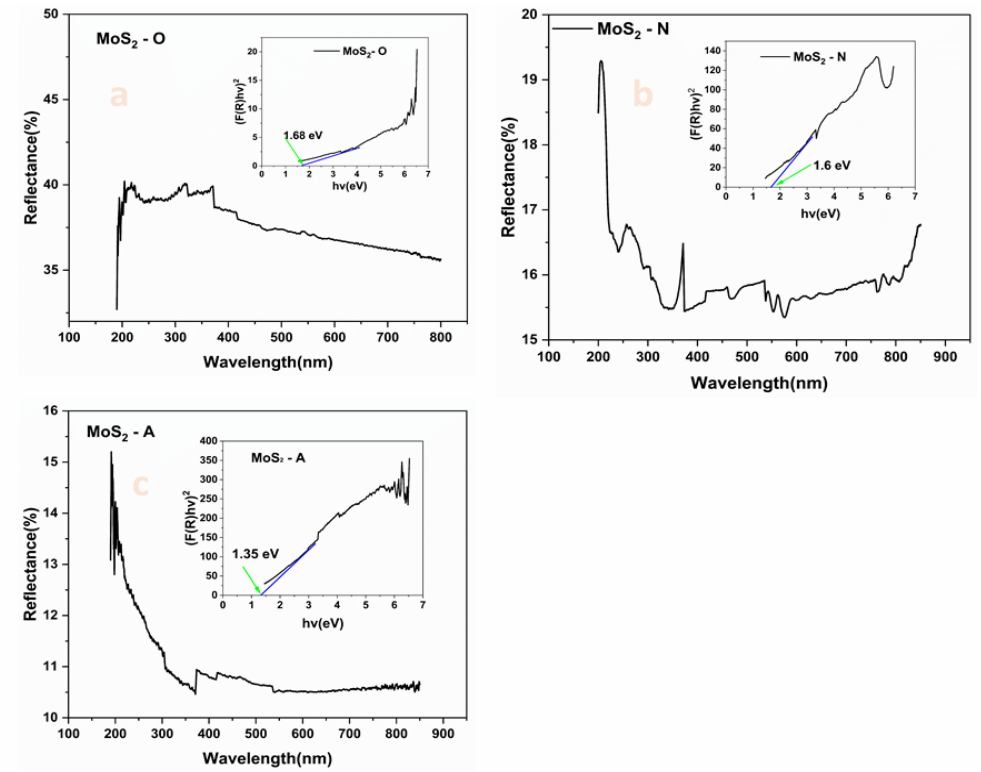

Figure 5:UV -Vis diffuse reflectance spectra of (a) MoS_2-O, (b) MoS_2-N and (c) MoS_2-A

VI. UV-Vis Diffuse Reflectance Spectroscopy

The synthesized samples are studied for their optical properties using diffuse reflectance spectroscopy.Diffuse reflectance spectroscopy(DRS) study is used to calculate the optical band gap of synthesized samples. The reflectivity patterns of samplesMoS_2(O), MoS_2(N) and MoS_2(A),are shown in figure 5(a, b, c). Figure 5 depicts the band gap values, which are calculated using Kubelka-Munk theory. In Kubelka Munk Theory: The Kubelkamunk function (F(R)) is used to transform reflectance spectra to absorption spectra(equation 3)**[13]**

where

$(F(R)hv)^{1/n} = B(hv-E_g)$ ---------- (3)

where R = reflectance,

v = frequency of photon,

Eg = energy band gap value,

h = Planck's constant,

B = constant.

The value of n is ½ for direct and 2 for indirect electron transition. The embedded graphsshown in Figure 5were plotted with F(R) and hv, taking n values equal to ½. The band gap value is obtained by extrapolating the graph. The obtained values are to be 1.68 eV, 1.6 eV, and 1.35eV forMoS_2 (O), MoS_2(N) and MoS_2(A) respectively. All band gap values lie in the visible region. The lower value of MoS_2(A) among all three indicates better performance towards electrochemical processes.

.

VII. Cyclic voltammetry

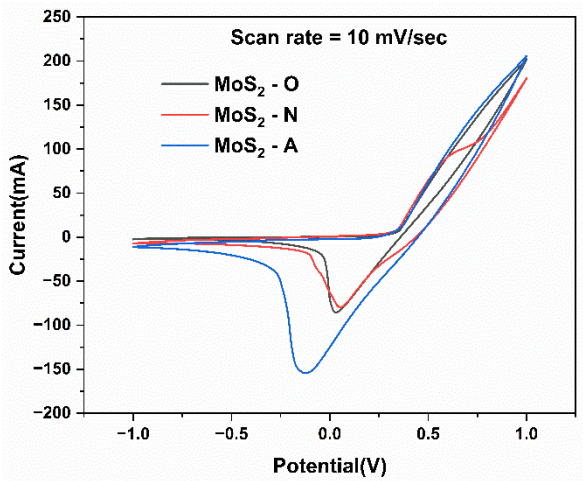

Figure 6: Cyclic voltammetry (CV) curve of (a) MoS_2-O, (b) MoS_2-N and (c) MoS_2-A

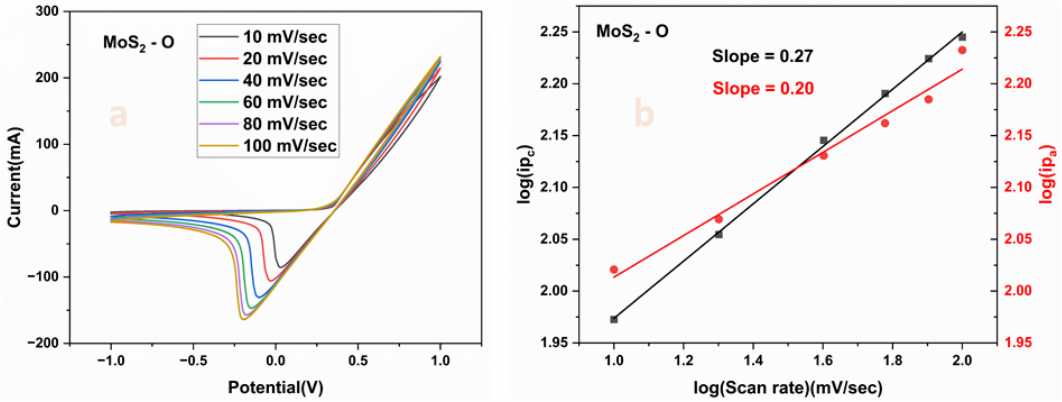

Figure 7:CV curve and variation of log current (cathodic & anodic) wrt log scan rate of (a) MoS_2-O

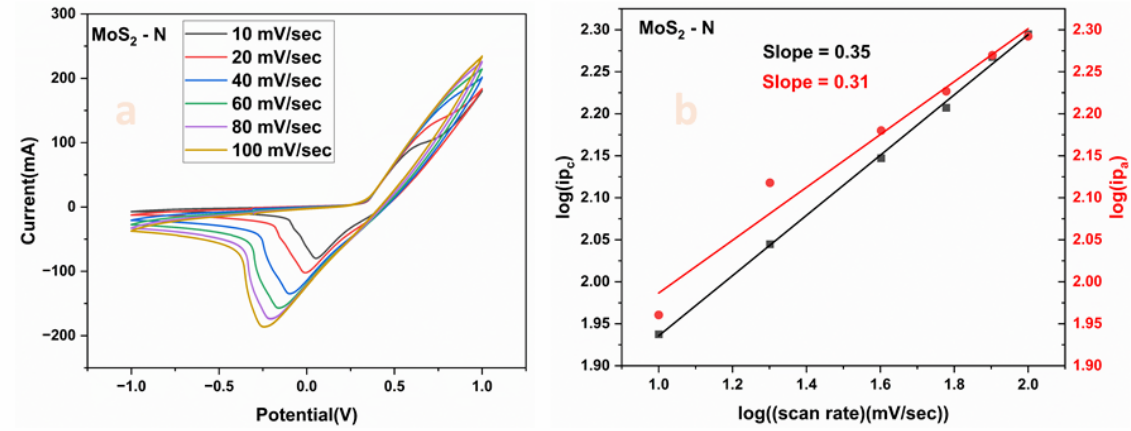

Figure 8:CV curve and variation of log current (cathodic & anodic) wrt log scan rate of MoS_2-N

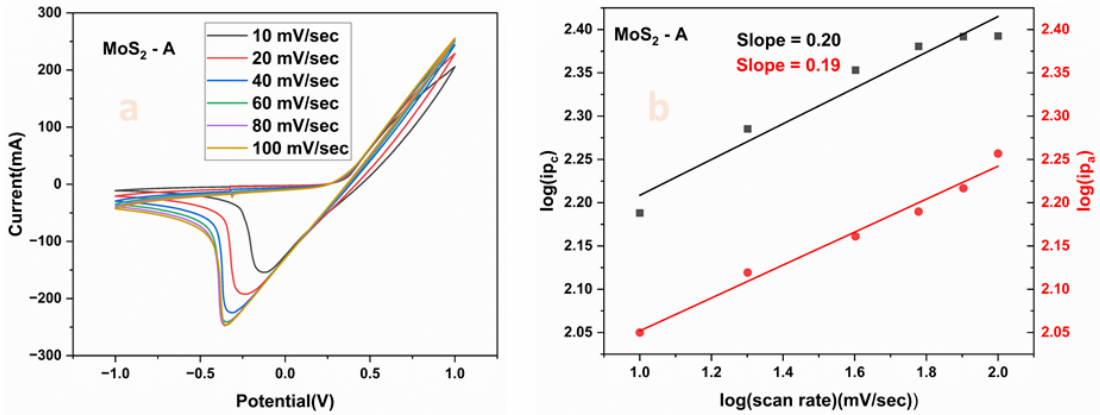

Figure 9:CV curve and variation of log current (cathodic & anodic) wrt log scan rate of MoS_2-A

Cyclic voltammetry technique was used to analyze the performance of the working electrode towards the specific capacitance.1 M KOH in DI water was taken to prepare the electrolyte for the analysis. The cyclic voltammetry technique was conducted using a three-electrode system, out of which one is the working electrode of material made of nickel foam and the other two are calomel and platinum, which serve as reference and counter electrodes. The potential window was set in the range of -1 to 1 volt. The cyclic voltage graph of synthesised samples is shown in figures (7(a),8(a),9(a)). These curves represent the variation of current wrt applied voltage. As the voltage increases, positive side oxidation occurs and current reaches its maximum value at a potential of 1 volt. After that, reduction starts, and current reaches its maximum value at -1 volt. Two redox peaks—one is an anodic peak on the oxidation side and another is a cathodic peak on the reduction side—occur, which indicates the charge storage mechanism. All the prepared samples show both anodic and cathodic peaks, confirming the occurrence of a redox reaction. Further, all these curves are scanned at rates of 10, 20,40,60,80,100mV/sec.As the scan rate increase, current increases. This increase in current with an increase in scan rate arises due to the quick exchange of redox ions at electrode material, representing the super capacitivebehaviour of material. Also, the shift in cathodic peak towards negative and anodic peak towards positive occurred because of the diffusion-controlled process**[14]**. The log current versus log scan rate plot is depicted in figures (7(b), 8(b) and 9(b)). These curves are straight lines with slope values of 0.27, 0.35 and 0.20 for cathodic while 0.20 ,0.31 and 0.19 for samples MoS_2 (O), MoS_2(N) and MoS_2(A) respectively. These slope values give the type of process involved during electrochemical reaction based on the concept of power law(equation 4), which **is[15]**

$$I=av^b \qquad \text{----------(4)}$$

where i = redox peak current,

v = scan rate

taking log of equation 4

$$\log I = \log a + b\log v \qquad \text{----------(5)}$$

Here the b value is the slope of the equation 5. The value of b determines the type of reaction mechanism that occurred during the electrochemical reaction. The value of b nearer to 1 indicates the capacitive behaviour, and

close to 0.5 is related to a diffusion-controlled process. Now according to power law, all three samples, MoS_2 (O), MoS_2(N) and MoS_2(A) exhibit the diffusion-controlled process.

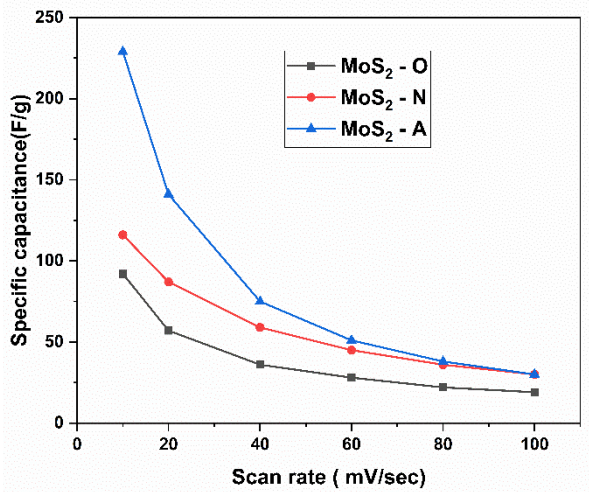

Figure 10: Variation of specific capacitances of (a) MoS_2-O, (b) MoS_2-N and (c) MoS_2-A wrt scan rate

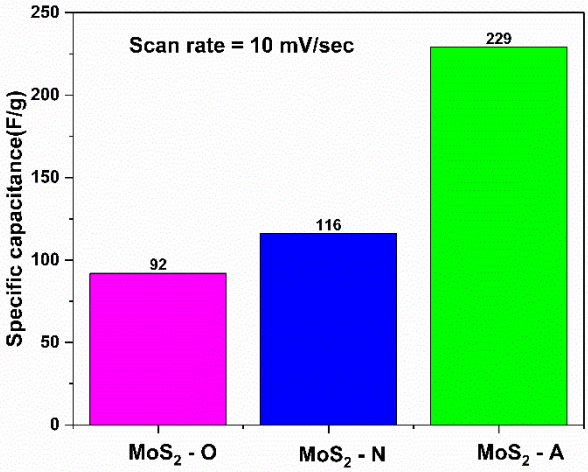

Figure 11: Comparison of specific capacitances of (a) MoS_2-O, (b) MoS_2-N and (c) MoS_2-A at scan rate 10mV/sec

Specific capacitance value of all synthesized samples was calculated using the formula(6)**[16]**

----------(6)

= Area under CV curve

= Scan rate

= Potential window

Figure 10illustrates the supercapacitance value of synthesized samples wrt scan rate. Scan rates are varied from 10 mV/sec to 200 mV/sec in a regular interval of 20. From the figure, it was observed that specific capacitance decreased as the scan rate increased. This type of behaviour was observed because, at a lower scan rate, more ions from the electrolyte solution were diffused into the interlayer of active electrode material, which further enhanced the charge transfer reaction. While at a higher scan rate, electrochemical processes slow down due to insufficient time available for the diffusion of ions into the electrode material.

Further, we compared the specific capacitance values of samples MoS_2 (O), MoS_2(N) and MoS_2(A) at a fixed scan rate of 10 mV/sec. Figure 11 depicts that sample MoS_2(A) showed the highest specific capacitance(229 F/g) in comparison to MoS_2 (O)(92 F/g) and MoS_2(N)(116 F/g). In MoS_2(A) samplehave more catalytic active site for the transfer of charged ions to the electrode surface. Also, the high-rich Ssites in the MoS_2(A) sample provide active sites for electrochemical reactions, which further enhanced the specific capacitance.

VIII. Conclusion

1T/2H MoS_2 nanoflowers were successfully synthesized using oxalic, nitric, and ascorbic acids as reducing agents. The as-prepared materials were utilized to prepare electrodes for electrochemical study. The results of electrochemical analysis showed that the MoS_2 nanoflower prepared using ascorbic acid showed the highest specific capacitance of 229 F/g in comparison to the material prepared using oxalic and nitric acid. This study shows that MoS_2prepared using ascorbic acid as a reducing agent can be further used in electrochemical energy storage devices in the future.

Declaration of Competing Interests:The authors declare that they have no known competing financial interest.

Declaration of Funding Statement: There is no specific grant from any funding agency.

Data Availability Statement: Data will be provided when asked.

Acknowledgements:The authors are thankful to the vice chancellor (Prof Anand Srivastava), NSUT for providing the infrastructure and essential resources.

References:

[1]. Ang TZ, Salem M, Kamarol M, Das HS, Nazari MA, Prabaharan N. A comprehensive study of renewable energy sources: Classifications, challenges and suggestions. Energy Strategy Reviews. Elsevier; 2022 Sep 1;43:100939.

[2]. Paraschiv LS, Paraschiv S. Contribution of renewable energy (hydro, wind, solar and biomass) to decarbonization and transformation of the electricity generation sector for sustainable development. Energy Reports. Elsevier; 2023 Sep 1;9:535–44.

[3]. Rudra S, Seo HW, Sarker S, Kim DM. Supercapatteries as Hybrid Electrochemical Energy Storage Devices: Current Status and Future Prospects. Multidisciplinary Digital Publishing Institute (MDPI); 2024 Jan 1;29(1):243.

[4]. Liu Y, Jiang SP, Shao Z. Intercalation pseudocapacitance in electrochemical energy storage: recent advances in fundamental understanding and materials development. Materials Today Advances. Elsevier; 2020 Sep 1;7:100072.

[5]. Hayat M, Abdullah M, Jabbour K, Bibi N, Khan S, Ali B, et al. Facile synthesis of 2-D rGO based SmSe nanohybrid via hydrothermal route for solid-state supercapacitor. Materials Chemistry and Physics. Elsevier; 2023 Dec 1;310:128436.

[6]. Liang X, Chen Y, Jiao Z, Demir M, Du M, Han J. MXene-transition metal sulfide composite electrodes for supercapacitors: Synthesis and electrochemical characterization. Journal of Energy Storage. Elsevier; 2024 May 30;88:111634.

[7]. Ismail KBM, Arun Kumar M, Mahalingam S, Kim J, Atchudan R. Recent Advances in Molybdenum Disulfide and Its Nanocomposites for Energy Applications: Challenges and Development. Materials 2023 Jun 19 ;16(12):4471.

[8]. Pradhan G, Sharma AK. Temperature controlled 1T/2H phase ratio modulation in mono- and a few layered MoS2 films. Applied Surface Science. North-Holland; 2019 Jun 15;479:1236–45.

[9]. Abinaya R, Archana J, Harish S, Navaneethan M, Ponnusamy S, Muthamizhchelvan C, et al. Ultrathin layered MoS2 nanosheets with rich active sites for enhanced visible light photocatalytic activity. RSC Advances ,The Royal Society of Chemistry; 2018 Jul 24 ;8(47):26664–75.

[10]. Khandare LN, Late DJ, Chaure NB. MoS2 nanobelts-carbon hybrid material for supercapacitor applications. Frontiers in Chemistry [Internet]. Frontiers Media SA; 2023 Oct 26;11:1166544.

[11]. Lee S, Hwang J, Kim D, Ahn H. Oxygen incorporated in 1T/2H hybrid MoS2 nanoflowers prepared from molybdenum blue solution for asymmetric supercapacitor applications. Chemical Engineering Journal. Elsevier; 2021 Sep 1;419:129701.

[12]. Nayak D, Kumar A, Thangavel R. Synthesis of MoS2 Nanoflowers for Photocatalytic Degradation of Organic Dyes. ACS Applied Nano Materials [Internet]. American Chemical Society; 2023 Oct 27 [cited 2024 Jun 23];6(20):19476–90.

[13]. Panchu SJ, Raju K, Swart HC, Chokkalingam B, Maaza M, Henini M, et al. Luminescent MoS2Quantum Dots with Tunable Operating Potential for Energy-Enhanced Aqueous Supercapacitors. ACS Omega,American Chemical Society; 2021 Feb 23;6(7):4542–50.

[14]. Haque F, Rahman M, Ahmed E, Bakshi P, Shaikh A. A Cyclic Voltammetric Study of the Redox Reaction of Cu(II) in Presence of Ascorbic Acid in Different pH Media. Dhaka University Journal of Science. Bangladesh Journals Online (JOL); 2013 Nov 18;61(2):161–6.

[15]. Nawaz S, Khan Y, Khalid S, Malik MA, Siddiq M. Molybdenum disulfide (MoS2) along with graphene nanoplatelets (GNPs) utilized to enhance the capacitance of conducting polymers (PANI and PPy). RSC Advances, The Royal Society of Chemistry; 2023 Sep 26;13(41):28785–97.

[16]. Singha SS, Rudra S, Mondal S, Pradhan M, Nayak AK, Satpati B, et al. Mn incorporated MoS2 nanoflowers: A high performance electrode material for symmetric supercapacitor. Electrochimica Acta. Pergamon; 2020 Apr 1;338:135815.